Chapter 6
Resonances in Electron Collisions with Small Biomolecules Using the R-Matrix Method

Lilianna Bryjko, Amar Dora, Tanja van Mourik, and Jonathan Tennyson

Abstract It is now widely accepted that collisions with low-energy electrons are the major cause of radiation damage in living cells and that it is the capture of these electrons into long-lived quasi-bound states, resonances, that is responsible for this damage. We have undertaken a set of systematic calculations using the UK Molecular R-matrix codes to study electron collisions with DNA and RNA bases. Here we summarise the results of our calculations for electron collisions with adenine, guanine, uracil, cytosine and thymine. These studies aim to characterize not only low-lying shape resonances, which have been relatively well-studied, but also to detect longer-lived Feshbach resonances which are associated with simultaneous electronic excitation of the target molecule. The results of these calculations are dependent on the model chosen: only the more sophisticated, and computationally expensive, models give Feshbach resonances.

6.1 Introduction

The processes that follow the creation of thousands of low-energy electrons are now recognised as being extremely important [8]. These electrons are stripped off from molecules in the cell either directly by radiation or else by its first products, highly energetic primary electrons that can cause electron-impact ionisation. As a result, in the past few years, a growing literature has emerged concerning the damage to

L. Bryjko • T. van Mourik
EaStCHEM School of Chemistry, University of St Andrews, North Haugh,
St. Andrews, Fife KY16 9ST, UK
e-mail: lilabe@o2.pl; tanja.vanmourik@st-andrews.ac.uk

A. Dora • J. Tennyson (✉)
Department of Physics and Astronomy, University College London,
Gower St., London WC1E 6BT, UK
e-mail: amardora@gmail.com; j.tennyson@ucl.ac.uk

G.G. Gómez-Tejedor and M.C. Fuss (eds.), *Radiation Damage in Biomolecular Systems*, Biological and Medical Physics, Biomedical Engineering,
DOI 10.1007/978-94-007-2564-5_6,

nucleic acids by low-energy electrons (LEE) with energies between 0 and 20 eV [1, 4–8, 12, 18, 20, 30, 33–36, 38, 39, 57] produced by ionising radiation.

The mechanism of DNA-LEE interaction is important because the low-energy secondary electrons are the most abundant radiolysis species generated following the impact of high-energy radiation [12, 31, 32] and therefore highly pertinent to issues such as radiation damage and the development of radio therapy. Nucleic acids can be ionised and damage produced through the dissociation of the anion when the electron energy is higher than the ionisation threshold for DNA (between 7.85 and 9.4 eV, as measured for the DNA bases [22]). If the electron energy is lower, damage can still be generated, but through a negative anion-mediated mechanism, which starts with the capture of the electron in a molecular resonance, followed by the transfer of energy and electron density towards a weak bond that subsequently ruptures.

There are many controversial issues that concern the location of the initial capture site [8, 40], the dynamics of the metastable anion generated by electron capture (called transient molecular anion), and the identification of the final bond that ruptures [5–7, 23, 27–29, 41, 57].

There is a wide agreement that the electron capture is mainly due to the DNA and RNA bases, because these molecules have extended aromatic systems. The scattering electron can temporarily be captured by an unoccupied π^* orbital giving rise to a shape resonance [1, 5, 25]. When scattering is connected with electron excitation, Feshbach or core-excited resonances can occur. It has been suggested that electron attachment to the phosphate group also contributes to DNA strands breaks [5, 6, 28, 37].

Simons and co-workers [5–7] performed model calculations which showed that electrons with energies of about 1.0 eV can attach to a base to form a π^* anion, which then can break a σ bond connecting the phosphate to a sugar group. Li et al. [21] performed calculations on a sugar-phosphate-sugar model system using the ONIOM layer method and found that the activation barrier for bond rupture of the anion's phosphate-sugar C–O bond is only 0.5 eV, indicating that very-low-energy electrons can induce DNA strand breaks. Berdys at al. [6, 7] found that near zero energy, electrons may not easily attach directly (i.e. vertically) to the phosphate units, but can produce a metastable P = O π^* anion above 2 eV.

Resonances were observed by Pan et al. [27, 28] in linear and super-coiled DNA. They also observed desorption of H^- as the result of temporary capture of electrons by the bases, with a small contribution from a core-excited resonance on the sugar group, OH^- desorption by the localisation of electrons on the protonated form of the phosphate group, and production of O^- via the temporary localisation of electrons on the π^* double bond of the phosphate group. Pan and Sanche [29] measured dissociative-electron attachment (DEA) to the monosodium salt of phosphoric acid, Na_2PO_4, in the condensed phase, confirming DNA damage can be induced by low-energy electrons. A single broad peak whose maximum fell at 8.8, 8.0 or 7.3 eV, depending on whether the anion detected was H^-, O^-, or OH^-, was observed. König et al. [19] measured DEA spectra for the dibuthyl and triethyl phosphate ester, and observed a variety of anionic fragments. Using dibuthyl phosphate they found

that the compound undergoes effective DEA within a low-energy resonant feature at 1 eV and a further resonance peaking at 8 eV. The DEA reactions are associated with the direct cleavage of the C-O and the P-O bonds but also the excision of the PO^-, PO_3^- and $H_2PO_3^-$ units. They propose that the most direct mechanism of single strand breaks occurring in DNA is due to DEA directly to the phosphate group.

Low-energy electron collisions with molecules can result in a variety of different processes [46]. A common feature of all these processes is that they can be considered to go via an intermediary, AB^-. One of the methods used to consider low-energy electron-molecule collisions is the R-matrix method [10, 11, 45], which is built around obtaining accurate wave functions for this intermediary and hence gives a theoretical framework capable of modelling all the above processes.

In this chapter we describe the application of R-matrix calculations to DNA and RNA constituents. A particular advantage of this method is its ability to treat not only shape resonances, which have been widely studied by a variety of methods, but also Feshbach resonances. Feshbach resonances have been found to be important experimentally [2, 3] but have received much less attention theoretically.

The size of these molecules and, in particular, the complexity of their electronic wavefunctions makes such calculations very challenging. So far the study of each system has necessitated the consideration of a number of models in order to obtain reliable results. We have completed studies on electron collisions with uracil [13], phosphoric acid [9], adenine, guanine, cytosine and thymine which consider these issues in turn for each molecule. Here, instead, we present a set of results for electron collisions with the bases calculated using a single model, which facilitates intercomparison between these species.

6.2 The R-matrix method

The basis of our calculations is the R-matrix method. The topic of electron-molecule collision calculations has been extensively reviewed by one of us [45] and only a flavor of the method will be given here.

The underlying physical model used in R-matrix calculations is the division of space into an inner region, contained within a sphere of radius a and centered on the target center-of-mass, and an outer region. The inner region is designed to be large enough to contain the entire electron density of the molecular target, including those for excited states in calculations which consider electronic excitation. This can be an issue for the biomolecules considered since they are considerably larger than the small molecules traditionally studied using this methodology. In the inner region the scattering electron and target electrons are treated as being indistinguishable and all interactions, including electron-electron correlation and exchange, are explicitly considered. Conversely, in the outer region the scattering electron is only affected

by the long-range potential of the target. As all the molecules considered here have permanent dipole moments, the long-range effect of the resulting dipole potentials need to be treated.

The R-matrix, which relates the scattering wavefunctions to its derivative at a given distance, is constructed on the boundary of the inner and outer region. The R-matrix itself is energy-dependent but can be built from the results of energy-independent inner-region calculations. This has the significant advantage that the energy dependence is entirely obtained from rapid, outer-region calculations. This is particularly useful for calculations aimed at characterizing resonances since such calculations usually require the use of a dense grid of energies.

In this work the R-matrix method is used to obtain the eigenphase sums. To obtain resonance positions and widths, these eigenphase sums were automatically fitted to a Breit-Wigner form by the recursive resonance fitting [47]. The calculations also give elastic electron collision cross sections and, for models which include electronically excited states in the close-coupling expansion, electron impact electronic excitation cross sections.

The UK Molecular R-matrix codes [26] are designed to be very flexible and a number of models have been tested in the course of the work considered here. The simplest of these models is the so-called static exchange (SE) approximation in which a full collision treatment is used for a target which is not allowed to relax during the collision. Polarisation effects can be included using the static exchange plus polarisation (SEP) approximation which allows for single excitations of the target wavefunction. The only resonances that can be detected in an SE calculation are shape resonances where the electron is temporarily trapped behind a centrifugal barrier. The SEP model moves these resonances to lower energy and also can, at least in principle, give Feshbach resonances. Feshbach resonances, which are associated with simultaneous electronic excitation of the target and trapping of the electron, are best given by calculations which explicitly include the parent target state(s) for a given resonance, These are best considered by using several states in a close-coupling (CC) expansion. Our best results presented below were all obtained using CC models.

The use of CC methods for molecules with many valence electrons, such as the ones considered here, leads to very large Hamiltonian matrices. That has led to the development of special methods for treating the problems both in terms of Hamiltonian construction [42] and diagonalisation [16, 44]. In particular the use of the so-called partitioned R-matrix [44] means that it is not necessary to explicitly obtain all the eigenvalues and eigenvectors of the scattering Hamiltonian. The CC results presented below are based on the use of all eigenvalues and vectors (typically 4000 to 6000) for "contracted" calculations but only the 5000 lowest solutions for "uncontracted" calculations which lead to very large Hamiltonian matrices, typically of dimension significantly bigger than 100 000.

The biomolecules considered here have also been the subject of R-matrix calculations by Tonzani and Greene [50]. The R-matrix method developed by these workers [48, 49] has significant differences from the one used by us. Their method involves using R-matrices to solve the electron-molecule scattering problem defined entirely by potentials. Even if one ignores the issue that interactions

such as exchange cannot be written as a simple, energy-independent potential, the method is only capable of performing calculations within the SE and SEP models.

6.3 Target calculations

The geometries of all DNA bases except uracil were determined using B3LYP/6-31+G* density functional theory and Gaussian 03 [24]. Except for thymine, the molecules were constrained to be in C_s symmetry. The geometry of uracil was optimised with the MP2 method and using a 6-31G* basis set as reported previously [52].

There are various issues in choosing a suitable target wavefunction for use in scattering calculations, which depend on what aspect of the problem is of interest. For the SE and SEP models the use of Hartree-Fock wavefunctions is standard; for CC calculations there is more choice. In particular these calculations usually attempt to represent several low-lying states of the target. This can be difficult given the constraints that all states must be represented by a single orbital set and that it must be possible to use in a balanced and tractable scattering calculation.

Our favoured method is to represent CC target wavefunctions using a complete active space (CAS) configuration interaction (CI) model. In the CAS-CI model, core electrons are frozen in the self-consistent field (SCF) orbitals and the active electrons are distributed amongst all the valence orbitals, subject only to the constraints of overall space-spin symmetry. This approach has significant advantages in terms of performing a balanced treatment between the target and the scattering wavefunction [43].

Even within the CAS-CI model there is considerable flexibility over the precise choice of molecular orbitals used. Here we use CAS-SCF orbitals generated by MOLPRO. Table 6.1 presents results for the bases considered. The calculations were performed using cc-pVDZ Gaussian Type Orbital (GTO) basis sets and an active space of 14 electrons in 10 orbitals for uracil, cytosine and thymine, 12 electrons in 10 orbitals for adenine and 12 electrons in 9 orbitals for guanine. Full details, including the actual configurations used, are given in Table 6.2. Besides the calculated energies for the ground and 15 lowest excited states, the table gives our calculated permanent dipole moment for each molecule. This property is important since the long-range nature of this moment has a strong effect on the scattering.

6.4 Scattering calculations

In the scattering calculations the target basis set was augmented with sets of GTOs with $\ell \leq 4$ (up to g-wave) to represent the continuum wavefunctions [14]. All calculations were performed for an R-matrix radius $a = 13\ a_0$ except those on thymine which used $a = 15\ a_0$.

Table 6.1 The CASSCF $X\ ^1A'$ (or $X\ ^1A$) ground state energies (in a.u.) and dipole moments (in Debye), and the relative energies (in eV) of the lowest 15 excited states of the nucleic acid bases

Adenine	Guanine	Uracil	Cytosine	Thymine
−464.6212766	−539.476656	−412.563491	−392.691128	−451.606027
4.61 ($^3A'$)	3.93 ($^3A'$)	3.87 ($^3A'$)	3.53 ($^3A'$)	3.86 (^3A)
5.47 ($^3A'$)	5.02 ($^3A'$)	4.75 ($^3A''$)	4.63 ($^3A'$)	4.85 (^3A)
5.87 ($^3A'$)	5.53 ($^3A''$)	4.92 ($^1A''$)	4.64 ($^3A''$)	5.03 (^1A)
6.13 ($^1A'$)	5.66 ($^1A''$)	5.49 ($^3A'$)	4.75 ($^1A'$)	5.54 (^3A)
6.39 ($^3A'$)	5.75 ($^3A'$)	6.29 ($^3A''$)	4.75 ($^1A''$)	6.36 (^3A)
7.09 ($^1A'$)	6.07 ($^1A'$)	6.36 ($^3A'$)	5.35 ($^3A''$)	6.38 (^3A)
7.34 ($^3A''$)	6.58 ($^1A'$)	6.49 ($^1A''$)	5.39 ($^3A'$)	6.56 (^1A)
7.41 ($^1A''$)	6.85 ($^3A''$)	6.59 ($^1A'$)	5.55 ($^3A''$)	6.62 (^1A)
7.82 ($^1A'$)	7.11 ($^1A''$)	7.00 ($^1A'$)	5.57 ($^1A''$)	7.20 (^1A)
7.85 ($^3A''$)	7.14 ($^3A'$)	7.70 ($^3A'$)	5.64 ($^1A''$)	7.78 (^3A)
8.09 ($^1A''$)	7.84 ($^3A''$)	7.78 ($^3A''$)	6.48 ($^1A'$)	7.92 (^3A)
9.38 ($^3A''$)	7.98 ($^1A''$)	7.89 ($^1A''$)	6.92 ($^3A'$)	7.98 (^1A)
9.43 ($^1A''$)	8.12 ($^3A''$)	7.93 ($^3A''$)	7.93 ($^3A'$)	7.98 (^3A)
11.21 ($^3A''$)	8.14 ($^1A''$)	7.96 ($^1A''$)	7.98 ($^3A''$)	8.05 (^1A)
11.23 ($^1A''$)	8.14 ($^1A'$)	8.56 ($^3A'$)	7.98 ($^1A''$)	8.71 (^1A)
3.06	1.58	4.06	6.33	3.96[a]

[a] Calculated ground state dipole moments.

Table 6.2 Configurations used in the CASSCF to generate the orbitals and in the final CAS-CI model

Molecule	CAS	Configurations
Adenine	(12,10)	(1a'-29a')^{58},(30a',1a"-9a")^{12}
Guanine	(12,9)	(1a'-30a')^{60},(1a"-3a")^{6},(31a',32a',4a"-10a")^{12}
Uracil	(14,10)	(1a' - 22a')^{44}, (23a', 24a', 1a" - 8a")^{14}
Cytosine	(14,10)	(1a' - 22a')^{44}, (23a', 24a', 1a" - 8a")^{14}
Thymine	(14,10)	(1a - 26a)^{52}, (27a- 36a)^{14}

In the course of this work we have performed many scattering calculations and this section will only summarise the results, see Table 6.3. In doing this we have chosen to select calculations performed in a uniform manner so that trends become apparent, rather than taking calculations individually optimized for each system. In particular we note that there are quite a number of ways of performing CC calculations. Of particular significance is the choice as to whether to "contract" or "uncontract" the configurations which involves placing the scattering electron in a target virtual orbital [43].

Although the difference between these two approaches may seem technical they actually differ quite significantly. The contracted method is standard but, without

Table 6.3 Low-lying resonant state positions (and widths) of the nucleic acid bases in eV

Bases	Models	$A''(\pi)$-resonances				$A'(\sigma)$-resonances		
Purine bases								
A	SE	3.23 (0.53)	4.02 (0.33)	5.06 (1.11)	10.62 (0.40)	9.85 (0.59)	10.60 (0.63)	
	SEP	1.30 (0.14)	2.12 (0.09)	3.12 (0.28)	7.07 (0.24)	8.60 (0.002)	8.87 (0.006)	
	CC	3.14 (0.42)	3.96 (0.31)	5.03 (0.62)	7.52 (0.22)	7.74 (1.21)	9.34 (0.38)	
	Ref. [51,55][a]	1.10	1.80	4.10				
	Obs. [1][b]	0.54	1.36	2.17				
G	SE	3.00 (0.33)	4.47 (0.35)	5.66 (0.80)	10.12 (1.26)	8.58 (0.21)	9.83 (0.39)	
	SEP	1.83 (0.16)	3.30 (0.24)	4.25 (0.33)	7.36 (0.27)	8.75 (0.004)	9.47 (0.004)	
	CC	1.68 (0.13)	3.19 (0.21)	4.74 (0.43)	6.96 (0.42)	6.44 (0.97)	7.49 (1.72)	
	Ref. [51,55][a]	1.55	2.40	3.75				
	Obs. [1][b]	0.46	1.37	2.36				
Pyrimidine bases								
U	SE	2.25 (0.26)	4.43 (0.41)	8.62 (2.69)		10.82 (3.13)		
	SEP	0.31 (0.015)	2.21 (0.16)	5.21 (0.72)		7.71 (0.01)	8.78 (0.01)	8.89 (0.01)
	CC	1.00 (0.05)	2.94 (0.29)	7.51 (2.38)				
	CC[c]	0.134 (0.0034)	1.94 (0.168)	4.95 (0.38)		6.17 (0.15)	7.62 (0.11)	8.12 (0.14)
	Ref. [52][d]	0.32 (0.018)	1.91 (0.16)	5.08 (0.40)		1.45	8.5	
	Obs. [1][b]	0.22	1.58	3.83				
C	SE	2.65 (0.34)	4.69 (0.67)	9.85 (2.08)		9.90 (0.61)		
	SEP	0.71 (0.05)	2.66 (0.33)	6.29 (0.72)		7.86 (0.003)		
	CC	1.20 (0.06)	3.02 (0.42)	6.08 (1.39)		6.38 (0.59)	6.51 (0.33)	
	CC[c]	0.36 (0.016)	2.05 (0.30)	6.04 (1.65)		6.64 (0.74)	6.87 (0.22)	
	Ref. [54,55][e]	0.50	2.40	6.30				
	Obs. [1][b]	0.32	1.53	4.50				

(continued)

Table 6.3 (continued)

Bases	Models	$A''(\pi)$-resonances		$A'(\sigma)$-resonances
T[f]	SE	2.46 (0.36)	4.60 (0.60)	9.12 (0.75)
	SEP	1.38 (0.19)	3.41 (0.16)	7.81 (0.18)
	CC	1.50 (0.15)	3.54 (0.19)	4.60 (1.86)
	CC[c]	1.21 (0.13)	3.25 (0.16)	5.42 (1.56)
	Ref. [54, 55][g]	0.30	1.90	5.70
	Obs. [1][b]	0.29	1.71	4.05

[a] Ref. [51, 55] used the SMC method with the SEP model. Only π resonance positions (and no widths) were reported for energies below 5 eV.
[b] Observed (ETS) resonance positions only.
[c] Uncontracted CC model, see Ref. [13].
[d] SMC calculation with the SEP model and forced C_s symmetry.
[e] SMC method with the SEP model. Only π resonance positions (and no widths) were reported.
[f] No symmetry employed in our thymine calculations because of the presence of the methyl group.
[g] Ref. [54] forced C_s symmetry in their thymine calculations. Used SMC method with the SEP model.

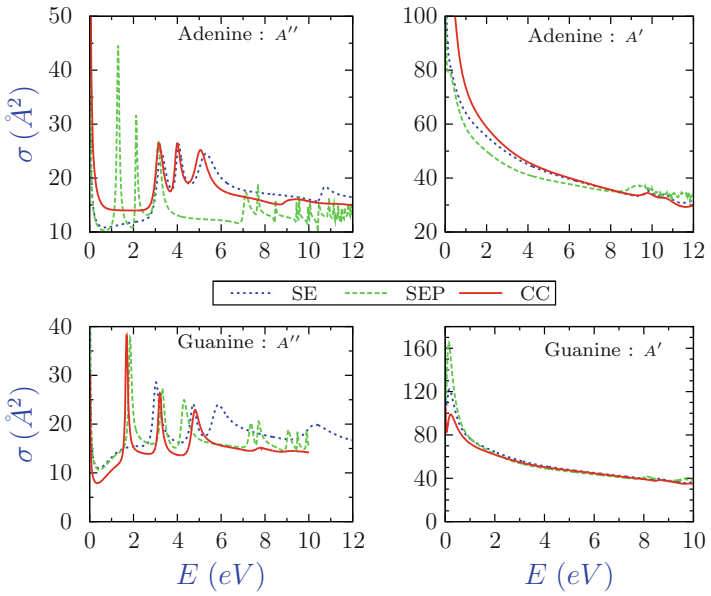

Fig. 6.1 Calculated elastic cross sections for the purine bases adenine and guanine. See text for details of the models used

performing exceptionally large CC expansions, tends to overestimate resonance positions. The uncontracted approach leads to systematically lower resonance positions. However it is not clear that this approach is completely balanced [43] and therefore it is possible to obtain resonances which are too low in energy or even become bound states. Furthermore, fully uncontracted calculations can become very large, requiring either unacceptably long times for the calculations or further compromises to be made on the size of the model wavefunctions chosen. For a more thorough discussion of the differences between these models, including full technical details, the reader is referred to our study on uracil [13]. The CC calculations reported here retained the lowest 32 states for uracil (U), 16 states for guanine (G), adenine (A) and thymine (T) and 20 states for cytosine (C).

Our previous study of resonances in phosphoric acid [9] revealed that the resonances showed little sensitivity to isomerisation. Our calculations suggest that this insensitively even extends between molecules with similar structures. Thus our calculations show a total of four π-type shape resonances for the purine bases, while the pyrimidines all have three.

The effect of these resonances can clearly be seen in the elastic cross sections. Figures 6.1 and 6.2 summarize our calculated elastic cross sections for the purine and pyrimidine DNA bases respectively. It should be noted that for strongly dipolar systems, such as the ones considered here, higher partial waves have a profound effect on the total elastic cross section, particularly at low energy. It is possible to correct for this using the Born approximation [56], which we have indeed done elsewhere [13]. However this correction is so big that it obscures the resonance

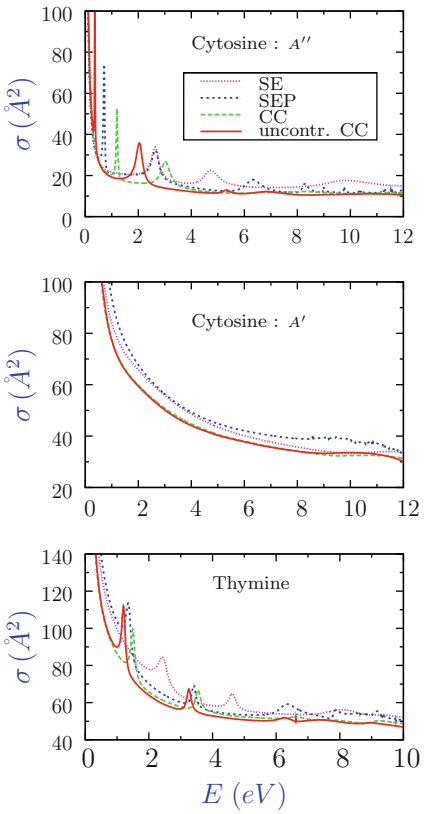

Fig. 6.2 Calculated elastic cross sections for the pyramidine bases cytosine and thymine

structures. For this reason the cross sections we present here are uncorrected. They are also, where possible, separated by symmetry to again emphasize the presence of the resonances.

6.5 Conclusion

This chapter summarizes our approach to identifying resonances in electron collisions with nucleic acid bases. The calculations presented here show that any of the nucleic acid base sites in DNA/RNA is capable of capturing low-energy electrons into π molecular orbitals to form a resonant π anionic state. This observation is in line with the suggestion that such π captures are followed by energy transfer to the σ molecular orbitals which in turn results in strand breaks [8].

A similar R-matrix approach to the one taken here has been used to consider resonances and electron collision cross sections in other biological important molecules such as phosphoric acid [9]. In this context it is worth noting that the R-matrix approach has been systematically applied to the study of low-energy

electrons with water, perhaps the most important biomolecule, obtaining results of exceptional accuracy [15]. However the only resonances supported by water are at relatively high electron impact energies [17] and are therefore unlikely to play a significant role in DNA strand breaks and other processes resulting in radiation damage.

Acknowledgements This project was funded by the UK Engineering and Physical Sciences Research Council. LB and TvM thank EaStCHEM for computational support via the EaStCHEM Research Computing Facility.

References

1. Aflatooni, K., Gallup, G.A., Burrow, P.D.: J. Phys. Chem. A **102**, 6205 (1998)
2. Antic, D., Parenteau, L., Lepage, M., Sanche, L.: J. Phys. Chem. **103**, 6611–6619 (1999)
3. Antic, D., Parenteau, L., Sanche, L.: J. Phys. Chem. B **104**, 4711–4716 (2000)
4. Bao, X., Wang, J., Gu, J., Leszczyński, J.: Proc. Natl. Aca. Sci. **103**, 5658 (2006)
5. Barrios, R., Skurski, P., Simons, J.: J. Phys. Chem. B. **106**, 7991 (2002)
6. Berdys, J., Anuszkiewicz, I., Skurski, P., Simons, J.: J. Am. Chem. Soc. **126**, 6441 (2004)
7. Berdys, J., Anuszkiewicz, I., Skurski, P., Simons, J.: J. Phys. Chem. A **108**, 2999 (2004)
8. Boudaiffa, B., Clutier, P., Hunting, A., Hules, M.A., Sanche, L.: Science **287**, 1658 (2000)
9. Bryjko, L., van Mourik, T., Dora, A., Tennyson, J.: J. Phys. B: At. Mol. Opt. Phys. **43**, 235203 (2010)
10. Burke, P.G., Berrington, K.A.: Atomic and Molecular Processes - An R-matrix Approach. Bristol and IOPP (1993)
11. Burke, P.G., Tennyson, J.: Mol. Phys. **103**, 2537–2548 (2005)
12. Cobut, V., Fongillo, Y., Patau, J.P., Goulet, T., Fraser, M.J., Jay-Gerin, J.P.: Radiat. Phys. Chem. **51**, 229243 (1998)
13. Dora, A., Bryjko, L., van Mourik, T., Tennyson, J.: J. Chem. Phys. **130**, 164307 (2009)
14. Faure, A., Gorfinkiel, J.D., Morgan, L.A., Tennyson, J.: Computer Phys. Comms. **144**, 224–241 (2002)
15. Faure, A., Gorfinkiel, J.D., Tennyson, J.: J. Phys. B: At. Mol. Opt. Phys. **37**, 801–807 (2004)
16. Galiatsatos, P.G.: (2010). Private communication
17. Gorfinkiel, J.D., Morgan, L.A., Tennyson, J.: J. Phys. B: At. Mol. Opt. Phys. **35**, 543–555 (2002)
18. Gu, J., Wang, J., Rak, J., Leszczyński, J.: Ang. Chem. **119**, 3549 (2007)
19. König, C., Kopyra, J., Bald, I., Illenberger, E.: Phys. Rev. Letts. **97**, 018105 (2006)
20. Kumar, A., Sevilla, M.D.: J. Phys. Chem. B **111**, 5464 (2007)
21. Li, X., Sevilla, M.D., Sanche, L.: J. Am. Chem. Soc **108**, 19013 (2004)
22. Lias, S.G., Levin, R.D., Kafafi, S.A.: In NIST Chemistry WebBook, NIST standard reference database number 69. National Institute of Stand ards and Technology, Gaithersburg, MD, httpand//webbook.nist.gov (2005)
23. Loos, P.F., Dumont, E., Laurent, A.D., Assfeld, X.: Chem. Phys. Lett. **475**, 120 (2009)
24. M. J. Frisch et al: (2004). Gaussian 03, Revision E.01, Wallingfort, CT
25. Martin, F., Burrow, P.D., Cai, Z., Clutier, P., Hunting, D., Sanche, L.: Phys. Rev. Lett. **93**, 068101 (2004)
26. Morgan, L.A., Tennyson, J., Gillan, C.J.: Computer Phys. Comms. **114**, 120–128 (1998)
27. Pan, X., Cloutier, P., Hunting, D., Sanche, L.: Phys. Rev. Letts. **90**, 208102 (2003)
28. Pan, X., Sanche, L.: Phys. Rev. Letts. **94**, 198104 (2005)
29. Pan, X., Sanche, L.: Chem. Phys. Lett. **421**, 404 (2006)

30. Panajotovic, R., Michaud, M., Sanche, L.: Phys. Chem. Chem. Phys. **9**, 138 (2007)
31. Pimblott, S.M., LaVerne, J.A.: Radiat. Res. **141**, 208 (1995)
32. Pimblott, S.M., LaVerne, J.A.: Radiat. Phys. Chem. **76**, 1244 (2007)
33. Ptasińska, S., Denifl, S., Gohlke, S., Scheier, P., Illenberger, E., Märk, T.D.: Angev. Chem., Int. Ed. **45**, 1893 (2006)
34. Ptasińska, S., Denifl, S., Scheier, P., Märk, T.D.: J. Chem. Phys. **120**, 8505 (2004)
35. Ptasińska, S., Sanche, L.: Phys. Chem. Chem. Phys. **9**, 1730 (2007)
36. Ptasińska, S., Sanche, L.: Phys. Rev. E **75**, 31915 (2007)
37. Rak, J., Kobylecka, M., Storoniak, P.: J. Phys. Chem. B **115**, 1911–1917 (2011)
38. Sanche, L., Schulz, G.: J. Phys. Rev. A **5**, 1672 (1972)
39. Scheer, A.M., Aflatooni, K., Gallup, G.A., Burrow, P.D.: Phys. Rev. Lett. **92**, 068102 (2004)
40. Shukla, M.K., Leszczyński, J. (eds.): Radiation Induced Molecular Phenomena in Nucleic Acids. Springer, Jackson (2007)
41. Takayanagi, T., Asakura, T., Motegi, H.: J. Phys. Chem. A **113**, 4795 (2009)
42. Tennyson, J.: J. Phys. B: At. Mol. Opt. Phys. **29**, 1817–1828 (1996)
43. Tennyson, J.: J. Phys. B: At. Mol. Opt. Phys. **29**, 6185–6201 (1996)
44. Tennyson, J.: J. Phys. B: At. Mol. Opt. Phys. **37**, 1061–1071 (2004)
45. Tennyson, J.: Phys. Rep. **491**, 29–76 (2010)
46. Tennyson, J., Gorfinkiel, J.D., Rozum, I., Trevisan, C.S., Vinci, N.: Radiat. Phys. Chem. **68**, 65–72 (2003)
47. Tennyson, J., Noble, C.J.: Computer Phys. Comms. **33**, 421–424 (1984)
48. Tonzani, S.: Computer Phys. Comm. **176**, 146–156 (2007)
49. Tonzani, S., Greene, C.H.: J. Chem. Phys. **122**, 014111 (2005)
50. Tonzani, S., Greene, C.H.: J. Chem. Phys. **124**, 054312 (2006)
51. Winstead, C., McKoy, V.: J. Chem. Phys. **125**, 244302 (2006)
52. Winstead, C., McKoy, V.: J. Chem. Phys. **125**, 174304 (2006)
53. Winstead, C., McKoy, V.: J. Chem. Phys. **125**, 074302 (2006)
54. Winstead, C., McKoy, V.: J. Chem. Phys. **127**, 085105 (2007)
55. Winstead, C., McKoy, V.: Rad. Phys. Chem. **77**, 1258 (2008)
56. Zhang, R., Faure, A., Tennyson, J.: Physica Scripta **80**, 015301 (2009)
57. Zheng, Y., Cloutier, P., Hunting, D.J., Wagner, J.R., Sanche, L.: J. Chem. Phys. **124**, 064710 (2006)